

Calculation and analysis of Mueller matrix in light scattering detection

Keding Yan (闫克丁)^{1*}, Shouyu Wang (王绶琦)¹, Shu Jiang (江舒)², Liang Xue (薛亮)³, Yuanyuan Song (宋媛媛)⁴, Zhengang Yan (闫振纲)⁵, and Zhenhua Li (李振华)^{1**}

¹Department of Information Physics & Engineering, Nanjing University of Science & Technology, Nanjing 210094, China

²704 Institute, China Shipbuilding Industry Corporation, Shanghai 200031, China

³College of Electronic and Information Engineering, Shanghai University of Electric Power, Shanghai 200090, China

⁴China North Vehicle Research Institute, Beijing 100072, China

⁵Xi'an Modern Control Technology Institute, Xi'an 710065, China

*Corresponding author: yankeding168@gmail.com; **corresponding author: lizhenhua@njust.edu.cn

Received April 3, 2014; accepted May 20, 2014; posted online August 22, 2014

A new criterion for target detection and identification is proposed to realize metal/dielectric identification and recognition based on Mueller matrix analysis. By using randomly rough surfaces as targets, numerical calculations are used to prove the robustness and accuracy of the criterion. Moreover, to the best of our knowledge, this is the first time to successfully explain the criterion by theoretical analysis. We believe the work provides an important reference for polarization imaging in laser radar and remote sensing, and so on.

OCIS codes: 290.5880, 240.5770, 290.0290, 240.0240.

doi: 10.3788/COL201412.092901.

Laser radar has become an important technique in a wealth of applications, such as remote sensing and target recognition, because of its high resolution, strong anti-interference, and small structure^[1,2]. Almost all laser radars detect targets according to the scattered lights from rough surfaces and studies of scattering from rough surfaces provide different methods for target detection and identification^[3,4]. Among these methods, detection based on light scattering intensity is a popular approach widely used in many laser radar applications for its simplicity and rapidness^[5]. It is found that both the refractive index and roughness of target surfaces influence the scattering intensity^[6]. However, single intensity parameter could not comprehensively reflect complete information of the targets which limits its potentiality in the future applications^[7,8].

In order to overcome the deficiency of the intensity detection, polarization detection is proposed which is able to provide more information of the target^[9,10]. We propose a new criterion based on Mueller matrix analysis to realize metals/dielectrics identification and recognition via polarization detection. By using different randomly rough surfaces as targets, we apply the Kirchhoff approximation (KA) method^[11,12] to calculate scattering which shows there is obvious difference in the Mueller matrix between dielectric and metal surfaces. KA has been widely used in both numerical simulation^[13,14] and experimental testing for realistic objects found in nature^[15,16]. Moreover, theoretical analysis is also proposed in this work, which proves that difference can be a robust and accurate criterion for metal/dielectrics detection. To the best of our knowledge, this is the first time to successfully explain the criterion by theoretical analysis.

KA is applied to calculate the Mueller matrix for light scattering from randomly rough surfaces. Compared with other numerical algorithms, such as the method of moment^[17-19] and the finite-difference time-domain method^[20,21], KA owns much higher calculation efficiency in time-consuming, besides, it is easy to set different polarization conditions. In order to simplify simulations, only one-dimensional (1-D) rough surfaces are used in this model.

There are mainly three steps in KA to calculate the Mueller matrix for light scattering from randomly 1-D rough surface. Firstly, the rough surfaces need to be generated with linear filtering method. Secondly, scattered fields are calculated via the Stratton-Chu equation from local fields of the rough surface solved by KA. After that, generating 1-D randomly rough surfaces repeatedly and the scattered fields with statistical stability could be achieved by solving the ensemble average of different scattered fields from different randomly rough surfaces. Finally, all elements in the Mueller matrix can be obtained from ensemble average of different scattered fields. Figure 1 reveals the whole procedures for calculating the Mueller matrix from rough surfaces.

The randomly rough surfaces could be generated by the sum of sinusoidal functions with different frequencies. Linear filtering method^[22] is applied to obtain these 1-D randomly rough surfaces as

$$f(x_n) = \frac{1}{L} \sum_{j=-N/2+1}^{N/2} F(k_j) \exp(ik_j x_n), \quad (1)$$

where x_n is the n th sampling point and $F(k_j)$ is the

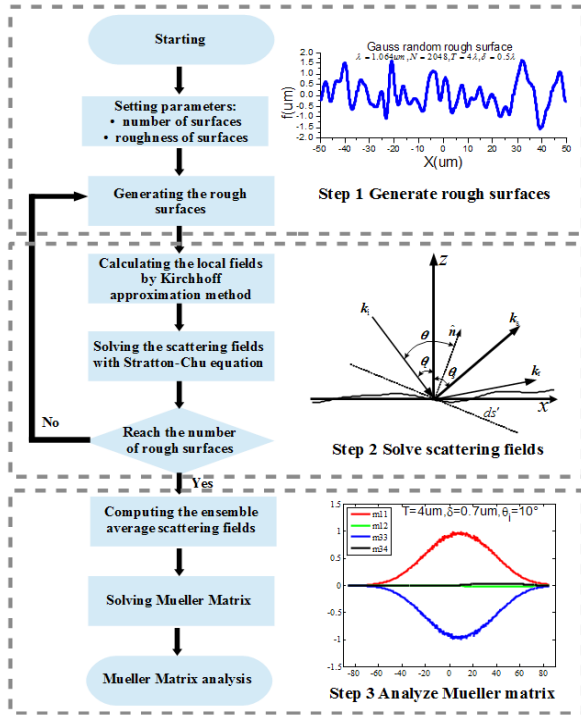


Fig. 1. Whole procedures for solving the Mueller matrix for light scattering by KA.

Fourier transform of surface distribution $f(x_n)$:

$$F(k_j) = \frac{2\pi}{\sqrt{2\Delta k}} \sqrt{S(k_j)} \begin{cases} [N(0,1) + iN(0,1)], j = -N/2 + 1, \dots, -1 \\ N(0,1), j = 0, N/2 \end{cases}, \quad (2)$$

where k_j is spatial frequency which equals $2\pi j/L$, L is length of the surface, Δk is the difference of spatial frequency, $N(0,1)$ is random number with Gaussian distribution, and $S(k_j)$ is the power spectral density of Gaussian distribution which is

$$S(k_j) = \delta^2 T / (2\sqrt{\pi}) \exp(-k_j^2/4). \quad (3)$$

By setting height RMS δ and correlation length T of randomly rough surfaces, and combining with Eqs. (1)–(3), 1-D randomly rough surfaces can be generated as shown in Step 1 of Fig. 1.

Next, we use Stratton–Chu equation to calculate the spatial scattered fields from the integral of local fields at each point on the rough surface^[23].

$$E^S(r) = \frac{1}{4\pi} \int_s \{ \hat{n} \times [\nabla \times E(r')] G(r, r') + [\hat{n} \times E(r')] \times \nabla G(r, r') + \hat{n} \cdot E(r') \nabla G(r, r') \} ds', \quad (4)$$

where r' is the vector in 1-D randomly rough surface and r is vector in the space, $E(r')$ is the local field at r' , \hat{n} is the normal vector of the local point, $G(r, r')$ is Green's function, ds' is the unit area of randomly rough surface, and $E^S(r)$ is the scattered field (Step 2 of Fig. 1).

KA is introduced as the boundary condition to calculate the local field on the rough surface. In the simulation, KA is applied to treat the local field at every point as the sum of the incident field and the reflective field from the tangent plane of that point. The incident wave is

$$E_i(r') = e_i \exp[ik_i \cdot r'], \quad (5)$$

where e_i and k_i are unit vector and wave vector of the incident wave, respectively. The reflective field can be calculated by the Fresnel reflective coefficient. Therefore, the local field of each local area is explained as

$$E(r') = [E_{si}(s_i + r_s s_r) + E_{pi}(p_i + r_p p_r)] \exp(ik_i \cdot r'), \quad (6)$$

where r_s and r_p are the Fresnel reflective coefficients in s- and p-polarizations, respectively; E_{si} and E_{pi} are amplitudes of s- and p-polarization incident waves; $s_i(s_r)$ and $p_i(p_r)$ are unit vectors perpendicular to and parallel with local incident (reflective) plane, respectively. Substituting Eqs. (5) and (6) into Eq. (4), the scattered fields $E^S(r)$ can be calculated.

The Mueller matrix can be calculated via the obtained scattered fields $E^S(r)$. The Stokes vectors of the incident light and scattered light are $S^I = (I^I, Q^I, U^I, V^I)^T$ and $S^S = (I^S, Q^S, U^S, V^S)^T$, respectively. According to O'Donnell and Knotts^[7], we have

$$S^S = MS^I \Rightarrow \begin{pmatrix} I^S \\ Q^S \\ U^S \\ V^S \end{pmatrix} = \begin{pmatrix} m_{11} & m_{12} & 0 & 0 \\ m_{12} & m_{11} & 0 & 0 \\ 0 & 0 & m_{33} & m_{34} \\ 0 & 0 & -m_{34} & m_{33} \end{pmatrix} \begin{pmatrix} I^I \\ Q^I \\ U^I \\ V^I \end{pmatrix}. \quad (7)$$

When the illuminating light is $+45^\circ$ linear polarization light, the Stokes vectors of the incident light are $S^I = (1, 0, 1, 0)^T$, while those of the scattered light are $S^S = (I^S, Q^S, U^S, V^S)^T = M \times (1, 0, 1, 0)^T = (m_{11}, m_{12}, m_{33}, -m_{34})^T$. Then, all the Mueller matrix elements could be solved as

$$M = \begin{pmatrix} m_{11} & m_{12} & 0 & 0 \\ m_{12} & m_{11} & 0 & 0 \\ 0 & 0 & m_{33} & m_{34} \\ 0 & 0 & -m_{34} & m_{33} \end{pmatrix} = \begin{pmatrix} I^S & Q^S & 0 & 0 \\ Q^S & I^S & 0 & 0 \\ 0 & 0 & U^S & -V^S \\ 0 & 0 & V^S & U^S \end{pmatrix}. \quad (8)$$

Based on KA and the Stratton–Chu equation, we have theoretically derived the Mueller matrix of 1-D randomly rough surface. It is found in 1-D randomly rough surface case that there are only four independent parameters in the Mueller matrix: m_{11} , m_{12} , m_{33} , and m_{34} . Thus, in the following numerical simulations, only these parameters are calculated and analyzed, which can reflect the characteristics of the rough surfaces.

In the numerical simulation, 10^5 1-D randomly rough surfaces are generated with a length of 100λ , λ is the wavelength of the incident light which is $1.064 \mu\text{m}$. We have calculated the Mueller matrix with different incident angles, roughness, materials, etc.

Firstly, we show the Mueller matrices of the dielectrics. Figure 2 shows the four independent elements in

the Mueller matrix of 1-D randomly rough dielectrics surface. The dielectric model is chosen as K5 glass with refractive index of 1.52^[24]. In the condition of dielectrics, refractive index is a real number which neglects the absorption of such materials. The four rows represent different wave incident angles which are 0°, 10°, 20°, and 30°, respectively. Different columns show different height RMS of randomly rough surfaces with the same correlation length 4λ .

Moreover, we have calculated LaSF30 glass with a refractive index of 1.80^[24] as shown in Fig. 3.

In Figs. 2 and 3, for dielectrics, the values of m_{11} and m_{33} are much larger than that of m_{12} . With the increase in roughness, m_{11} , m_{12} , and m_{33} are broadening obviously, while all m_{34} keep as zeros for dielectrics. Moreover, with the increase in the incident angles, the peaks of m_{11} , m_{12} , and m_{33} are all shifted according to the incident angles.

Besides, Mueller matrices of randomly rough metal surfaces are also calculated. We chose gold and iron surfaces as the targets. The refractive indexes at 1.064 μm of gold and iron are $0.1 + 6.54i$ and $3.24 + 4.26i$, respectively^[24]. The calculation results are shown in Figs. 4 and 5.

Similar to the randomly rough dielectric surfaces, with the increase in roughness, all elements from Mueller matrices of randomly rough metal surfaces are broadening. Besides, with the increase in the incident angles, the peaks of m_{11} , m_{12} , and m_{33} are all shifted according to the incident angles. These results can also be seen in our previous simulation work^[8].

There are no obvious differences in m_{11} , m_{12} , and m_{33} between dielectric and metal surfaces; however, in the

case of randomly rough metal surfaces, m_{34} is a nonzero value which is different from that of randomly rough dielectrics surfaces.

This obvious difference in the Mueller matrix could be applied as a criterion in polarization detection for metal and dielectric identification. In order to have deep understanding of the effect, we will use theoretical analysis to explain this obvious difference in the Mueller matrix elements between metals and dielectrics.

As shown in Step 2 of Fig. 1, when the incident and scattering angles, θ_i and θ_s are determined, scattered field is decided by both slope and reflective coefficients of local area in randomly rough surface. Major contributions for the scattered fields are those localized areas whose $s = dz/dx = \tan[(\theta_i - \theta_s)/2]$ and the probability density is^[8]

$$p(s) = \frac{1}{\sqrt{2\pi} \sigma/T} \exp\left(-\frac{s^2}{2(\sqrt{2} \sigma/T)^2}\right). \quad (9)$$

When the incident angle is decided, the reflective coefficients of the local areas are mainly dependent on the scattering angles and refractive index. Since the sample can be described by a constant complex valued refractive index, the reflective coefficients of p- and s-polarizations are shown as

$$r_p = \frac{n^2 \cos[(\theta_i + \theta_s)/2] - \sqrt{n^2 - \sin^2[(\theta_i + \theta_s)/2]}}{n^2 \cos[(\theta_i + \theta_s)/2] + \sqrt{n^2 - \sin^2[(\theta_i + \theta_s)/2]}}, \quad (10)$$

$$r_s = \frac{\cos[(\theta_i + \theta_s)/2] - \sqrt{n^2 - \sin^2[(\theta_i + \theta_s)/2]}}{\cos[(\theta_i + \theta_s)/2] + \sqrt{n^2 - \sin^2[(\theta_i + \theta_s)/2]}}, \quad (11)$$

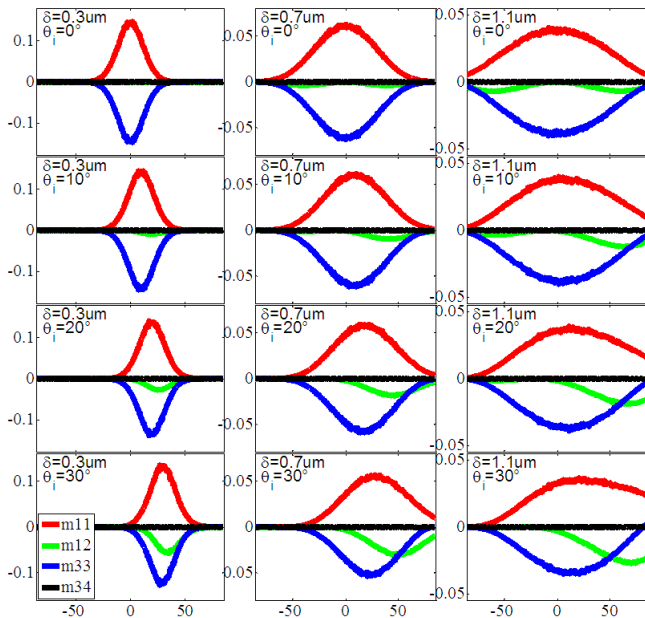


Fig. 2. Four independent elements in the Mueller matrix of the randomly rough K5 glass surfaces. The x -axis indicates scattering angle (unit: deg.) while the y -axis indicates intensity.

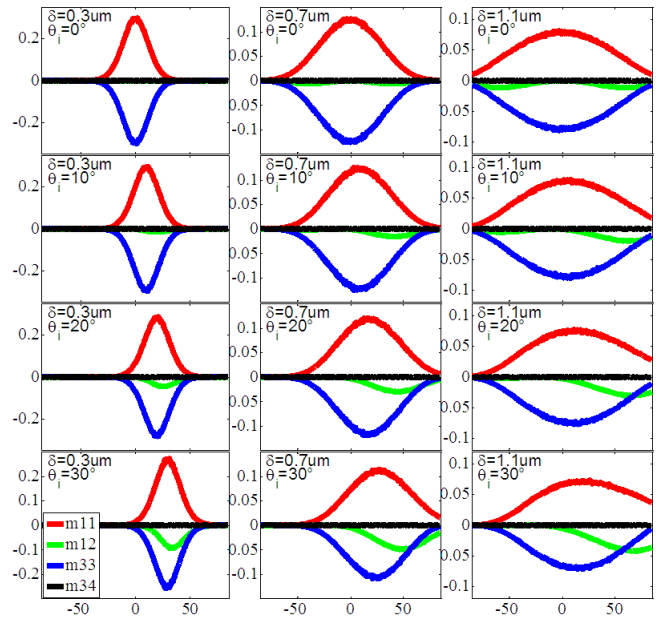


Fig. 3. Four independent elements in the Mueller matrix of the randomly rough LaSF30 glass surfaces. The x -axis indicates scattering angle (unit: deg.) while the y -axis indicates intensity.

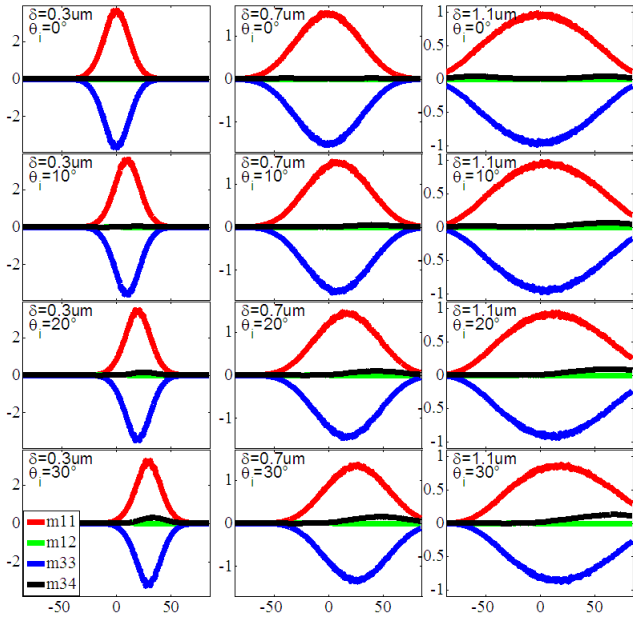


Fig. 4. Four independent elements in the Mueller matrix of the randomly rough gold surfaces. The x -axis indicates scattering angle (unit: deg.) while the y -axis indicates intensity.

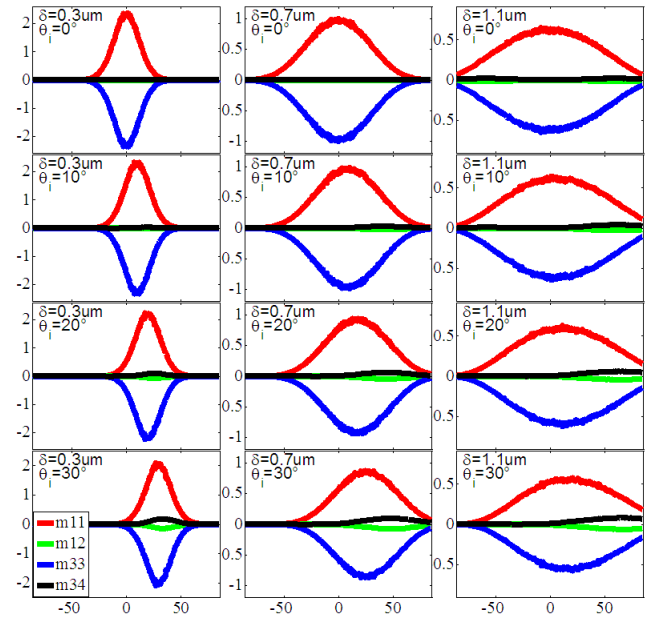


Fig. 5. Four independent elements in the Mueller matrix of the randomly rough iron surfaces. The x -axis indicates scattering angle (unit: deg.) while the y -axis indicates intensity.

where n is the refractive index. Assuming a $+45^\circ$ linear polarization wave whose amplitudes are perpendicular to and parallel with the incident plane are $A_{si}=1$ and $A_{pi}=1$, respectively, we use m'_{11} , m'_{12} , m'_{33} , and m'_{34} to express the Mueller matrix obtained by this theoretical analysis, which are

$$m'_{11} = \left[(A_{pi}r_p)(A_{pi}r_p)^* + (A_{si}r_s)(A_{si}r_s)^* \right] p(s), \quad (12)$$

$$m'_{12} = \left[(A_{pi}r_p)(A_{pi}r_p)^* - (A_{si}r_s)(A_{si}r_s)^* \right] p(s), \quad (13)$$

$$m'_{33} = \left[(A_{pi}r_p)(A_{si}r_s)^* + (A_{pi}r_p)^*(A_{si}r_s) \right] p(s), \quad (14)$$

$$m'_{34} = -i \left[(A_{pi}r_p)(A_{si}r_s)^* - (A_{pi}r_p)^*(A_{si}r_s) \right] p(s). \quad (15)$$

It is worth noting that all m'_{11} , m'_{12} , m'_{33} , and m'_{34} are real values. Figures 6 and 7 compare the numerical simulation and theoretical analysis of the four independent elements in the Mueller matrix of 1-D randomly rough surfaces. The results show that numerical calculations match well with those obtained from theoretical analysis, which illustrate the accuracy and robustness of the numerical calculation method used in the work.

From Figs. 6 and 7, it is obvious that the trends of m_{11} , m_{12} , and m_{33} are similar in both randomly rough dielectric and metal surfaces. Moreover, theoretical analysis also reflects the difference in the Mueller matrix parameters between randomly rough dielectrics

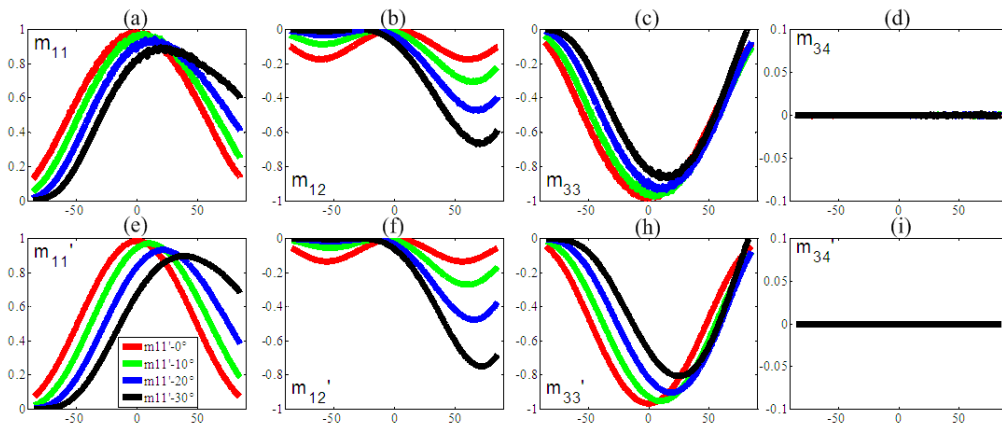


Fig. 6. Comparison between results of (a)–(d) numerical calculation and (e)–(i) theoretical analysis of randomly rough K5 glass surface in the Mueller matrix at different incident angles.

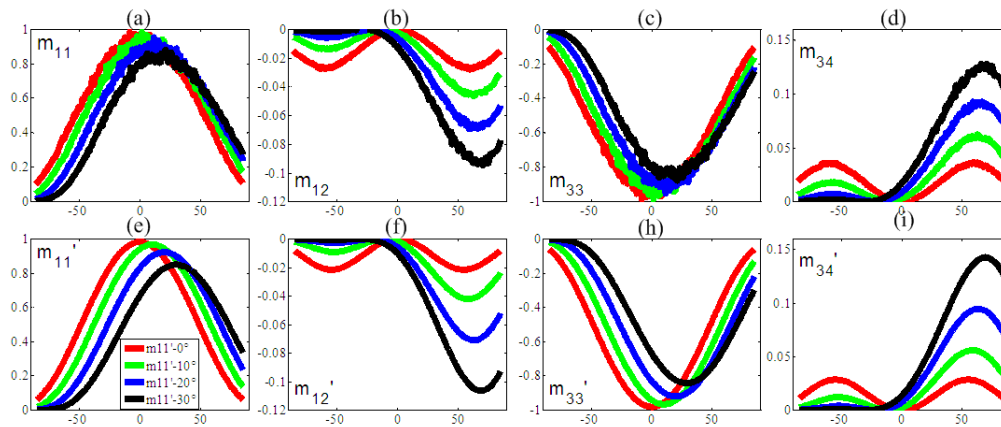


Fig. 7. Comparison between results of (a)–(d) numerical calculation and (e)–(h) theoretical analysis of randomly rough iron surface in the Mueller matrix at different incident angles.

and metal surfaces. In randomly rough dielectric surfaces, m_{34} keeps as zero, while in randomly rough metal surfaces, m_{34} owns the opposite form of the m_{12} as shown in Figs. 6(d), 6(i), 7(d) and 7(i).

The obvious difference in m_{34} is induced by the difference in Fresnel reflective coefficients in metals and dielectrics. As explained in Eq. (15), m_{34} is obtained by amplitudes and Fresnel reflective coefficients. Since the amplitudes in the theoretical are $A_{si}=1$ and $A_{pi}=1$, the Fresnel reflective coefficients play a main role in m_{34} modulation. For dielectrics, Fresnel reflective coefficients are all real numbers, therefore, m_{34} is zero according to Eq. (15). While for metals, their Fresnel reflective coefficients are complex numbers which generate nonzeros in m_{34} .

In addition, Fresnel reflective coefficients are decided by refractive index as shown in Eqs. (10) and (11). Since the refractive index of the material is independent of surface roughness, therefore, m_{34} in the Mueller matrix can be used as a robust criterion to distinguish metals and dielectrics based on the rough surface scattering. Besides, the Mueller matrix imaging is able to extract more information such as degree of polarization^[9] and mutual anisotropy^[25,26], which could be a potential guidance for target identification in laser radar and remote sensing.

In conclusion, we propose a new criterion to realize metal/dielectric identification and recognition based on scattered analysis. By studying m_{34} in the Mueller matrix, metals and dielectrics are well identified. Moreover, we prove the criterion is robust and owns potentials in laser radar and remote sensing, and so on.

References

1. S. Yoshikado and T. Aruga, *Appl. Opt.* **37**, 5631 (1998).
2. Z. Liu, R. Chen, N. Liao, and Y. Wang, *Chin. Opt. Lett.* **10**, 11201 (2012).
3. A. Ishimaru, *Proc. IEEE* **79**, 1359 (1991).
4. T. Mukai, A. Nakamura, and T. Sakai, *Adv. Space Res.* **37**, 138 (2006).
5. X. Zhu, J. Liu, D. Bi, J. Zhou, W. Diao, and W. Chen, *Chin. Opt. Lett.* **10**, 012801 (2012).
6. J. Sánchez-Gil and M. Nieto-Vesperinas, *J. Opt. Soc. Am. A* **8**, 1270 (1991).
7. K. O'Donnell and M. Knotts, *J. Opt. Soc. Am. A* **8**, 1126 (1991).
8. S. Jiang, C. Wang, J. Lai, B. Bian, J. Lu, and Z. Li, *J. Mod. Opt.* **58**, 1651, (2011).
9. F. Le Roy-Brehonnet and B. Le Jeune, *Prog. Quant. Electron* **21**, 109 (1997).
10. R. Ossikovski, *J. Opt. Soc. Am. A* **26**, 1109 (2009).
11. L. Guo, Y. Wang, and Z. Wu, *Chin. Opt. Lett.* **2**, 431 (2004).
12. J. Ma, L. Guo, and X. Cheng, *Chin. Opt. Lett.* **7**, 259 (2009).
13. N. Bruce, A. Sant, and J. Dainty, *Opt. Commun.* **88**, 471 (1992).
14. N. Bruce, V. Ruiz-Cortes, and J. Dainty, *Opt. Commun.* **106**, 123 (1994).
15. T. Kobayashi, H. Oya, and T. Ono, *Earth Plants Space* **54**, 983 (2002).
16. J. Chen, T. Lo, H. H. Leung, and J. Litva, *IEEE Trans. Geosci. Remote Sensing* **34**, 966 (1996).
17. R. Harrington, *Field Computation by Moment Method* (Macmillan, New York, 1968).
18. W. Chew, C. Lu, and Y. Wang, *J. Opt. Soc. Am. A* **11**, 1528 (1994).
19. I. Simonsen, A. Maradudin, and T. Leskova, *Phys. Rev. A* **81**, 013806 (2010).
20. S. Lee, C. Weng, M. Moghaddam, M. Nasir, S. Chuang, R. Herrick, and C. Balestra, *J. Lightwave Technol.* **9**, 1471 (1991).
21. F. Hastings, J. Schneider, and S. Broschat, *IEEE Trans. Antennas Propag.* **43**, 1183 (1995).
22. L. Tsang, J. Kong, K. Ding, and C. Ao, *Scattering of Electromagnetic Waves, Numerical Simulations* (Wiley, New Jersey, 2002).
23. J. Stratton, *Electromagnetic Theory* (Wiley, New Jersey, 2007).
24. M. Weber, *Handbook of Optical Materials* (CRC Press, Florida, 2002).
25. O. Arteaga, M. Baldrís, J. Antó, A. Canillas, E. Pascual, and E. Bertran, *Appl. Opt.* **53**, 2236 (2014).
26. V. Ushenko, O. Dubolazov, and A. Karachevtsev, *Appl. Opt.* **53**, B128 (2014).